Available online at www.sciencedirect.com
ScienceDirect
Trans. Nonferrous Met. Soc. China 24(2014) 491−498
Transactions of Nonferrous Metals Society of China
www.tnmsc.cn

# Density functional theory study on natural hydrophobicity of sulfide surfaces

Cui-hua ZHAO[1,2,3], Jian-hua CHEN[1,4], Bo-zeng WU[2], Xian-hao LONG[1]

1. School of Chemistry and Chemical Engineering, Guangxi University, Nanning 530004, China;
2. Guangxi China Tin Group Co., Ltd, Liuzhou 545006, China;
3. College of Materials Science and Engineering, Guangxi University, Nanning 530004, China;
4. College of Resources and Metallurgy, Guangxi University, Nanning 530004, China

Received 23 February 2013; accepted 28 July 2013

**Abstract:** Adsorption of water on sulfide surfaces and natural floatability of sulfide minerals were studied using density functional theory (DFT) method. All computational models were built in a vacuum environment to eliminate the effects of oxygen and other factors. $H_2O$ molecule prefers to stay with pyrite and sphalerite surfaces rather than water, whereas for galena, chalcocite, stibnite, and molybdenite, $H_2O$ molecule prefers to stay with water rather than the mineral surfaces. On the other hand, pyrite surface favors $N_2$ more than water, while sphalerite surface cannot adsorb $N_2$. These results show that galena, stibnite, chalcocite, and molybdenite are hydrophobic, while sphalerite is hydrophilic. Although pyrite has certain hydrophilicity, it tends to be aerophilic because the reaction of pyrite with $H_2O$ is weaker than pyrite with $N_2$. Thus, pyrite, galena, chalcocite, stibnite and molybdenite all have natural floatability.

**Key words:** sulfide minerals; water adsorption; natural floatability; density functional theory

## 1 Introduction

Flotation is a surface chemistry based process for the separation of fine solids, taking advantage of the difference in wettability of the solid particle surfaces. Hydrophobic surfaces solids are often naturally non-wettable by water. Such surfaces are also typically air attracting, known as aerophilic surface. They are strongly attracted to an air interface, readily displacing water on the solid surface. The floatability of minerals depends on the wettability degree of the surfaces with water. Over the last few decades, many studies have been performed on the natural floatability of certain sulfide minerals, but various researchers reached different conclusions [1−4]. For example, as early as 1940, RAVITZ [1] suggested that galena is naturally floatable; however, this premise has been object by other investigators [2−4]. Whether sulfides have natural floatability has been a controversial issue over the years.

FINKELSTEIN et al [4] and LEPETIC [5] observed natural floatability under certain conditions for chalcopyrite. HEYES and TRAHAR [6] showed that floatability in the absence of collectors occurs under oxidizing conditions and found that flotation could not be achieved under reducing conditions. GARDNER and WOODS [7] confirmed these observations with potentiostatic experiments. The presence of sulfur was suggested by these authors to be critical for chalcopyrite flotation in the presence of collectors. However, YOON [8] showed that chalcopyrite responds well to collectorless flotation process after sodium sulfide is added to the system. Sulfur was not detected on the chalcopyrite surface under these reducing conditions; thus, the natural floatability of sulfides depends on adsorption environment.

On the other hand, FUERSTENAU and SABACKY [9] studied the natural floatability of sulfide minerals (galena, chalcopyrite, chalcocite, pyrite and sphalerite) from various sources. The system used in this research was in an atmosphere containing less than $10^{-6}$ oxygen in mole fraction and water containing less than $5\times10^{-6}$ oxygen without addition of any collector or frother. The results showed that chalcocite, chalcopyrite, galena, and

**Foundation item:** Project (51164001) supported by the National Natural Science Foundation of China; Project (NCET-11-0925) supported by New Century Excellent Talents in University, China
**Corresponding author:** Jian-hua CHEN; Tel: +86-771-3232200; E-mail: jhchen1971@sina.com
DOI: 10.1016/S1003-6326(14)63087-9

pyrite are naturally floatable under specific conditions (low oxygen content, pH 6.8, no collector, no frother), which disagrees with the results reported [2−4]. According to results of FUERSTENAU and SABACKY [9], oxygen is a critical factor affecting the natural floatability of sulfide minerals. In the presence of oxygen, oxidation of the surfaces of these sulfides to sulfur-oxy species occurs. Under these conditions, water molecules are hydrogen bonded to the surface and the sulfide minerals lose their natural floatability.

Influence of oxygen on the process cannot be completely eliminated in any flotation system, and absolutely clean surface of minerals is hardly obtained in certain conditions and environments, which may result in differences in natural floatability of sulfide minerals observed by several investigators.

In recent years, a great deal of research for $H_2O$ adsorption on sulfide surfaces has been carried out. Our research group [10] studied the adsorption of water on sulfide surfaces (pyrite, sphalerite, galena and molybdenite) by microcalorimetry technique. The results showed that galena and molybdenite are hydrophobic, while pyrite and sphalerite are hydrophilic. The heat of adsorption is in decreasing order of pyrite, sphalerite, galena and molybdenite. The adsorption kinetics parameters of hydrophobic galena and molybdenite surfaces are close, while those of hydrophilic pyrite and sphalerite surfaces are very different. The adsorption rate of water on the sphalerite surface is larger than that of water on the pyrite surface. STIRLING [11] studied water interaction with the (100) surface of pyrite by means of ab initio molecular dynamics simulations. The results showed that a very strong preference for molecular adsorption on the surface iron sites. Hydrogen bonding plays an important role in the stabilization of the adsorbed water. Water forms a coordinative covalent bond with the surface iron. GUEVREMONT et al [12] investigated the interaction of water with atomically clean $FeS_2$ (100). The results showed that the binding sites on clean $FeS_2$ (100) can be broadly classified as being associated with stoichiometric $FeS_2$ (100) and a sulfur-deficient surface. These latter sites bind $H_2O$ more strongly than the former. WRIGHT et al [13] studied the reaction of water on the surface of PbS (galena). The results from both semi-empirical and ab initio levels of theory suggested that on a perfect (001), water is a stable species and dissociation does not occur. However, at a small step-like feature the reaction $PbS+H_2O\rightarrow Pb(OH)^{+}+HS^{-}$ is exothermic with a sufficiently low barrier that a facile reaction occurs at ambient temperature. ROSSO et al [14] studied the interaction of gaseous $O_2$, $H_2O$ and their mixtures with clean (100) surfaces of pyrite in ultra-high vacuum by scanning tunneling microscopy and spectroscopy (STM-STS), ultraviolet photoelectron spectroscopy (UPS) and ab initio calculations. The results indicated oxidative consumption of low binding-energy electrons occupying dangling bond surface states localized on surface Fe atoms, and the formation of Fe—O bonds. No such changes in the valence band spectra are observed for pyrite surfaces exposed to $H_2O$. The combined gases more aggressively oxidize the surface compared with equivalent exposures of pure $O_2$. Ab initio cluster calculations of adsorption energies and the interaction of $O_2$ and water species with the surface indicated that $H_2O$ dissociatively sorbs when $O_2$ is present on the surface. The study on ROSSO suggests that $O_2$ can be influential on $H_2O$ adsorption on sulfide surfaces.

In this work, $H_2O$ adsorption on sulfide surfaces and the natural hydrophobicity of sulfide minerals were studied by density functional theory (DFT) method. The sulfide minerals studied included pyrite, sphalerite, galena, chalcocite, stibnite and molybdenite. All calculations were carried out in the vacuum environment to completely eliminate the effects of oxygen and other similar factors.

## 2 Computational and experimental methods and models

### 2.1 Computational method

Based on the DFT method, all calculations were performed by CASTEP (Cambridge serial total energy package) program module developed by PAYNE et al [15], which is a first-principle pseudopotential method based on DFT. The DFT calculations have been performed using plane wave (PW) basis sets and ultrasoft pseudopotentials [16,17]. The exchange correlation functional used was the generalized gradient approximation (GGA), developed by PERDEW and WANG (PW91) [16]. The interactions between valence electrons and ionic core were represented with ultrasoft pseudopotentials. Valence electrons configuration considered in this study included Fe $3d^64s^2$, S $3s^23p^4$, Cu $3d^{10}4s^1$, Pb $5d^{10}6s^26p^2$, Sb $5s^25p^3$, Zn $3d^{10}4s^2$ and Mo $4s^24p^64d^55s^1$ states. Based on the test results, plane wave cut-off energies of pyrite and galena are 270 eV and 280 eV, respectively, and others (sphalerite, chalcocite, stibnite, molybdenite) are all 300 eV. The thicknesses of vacuum layer for all six sulfides are 15 Å, which is the most stable. The convergence tolerances for geometry optimization calculations were set to be the maximum displacement of 0.002 Å, the maximum force of 0.08 eV/Å, the maximum energy change of $2.0\times10^{-5}$ eV/atom and the maximum stress of 0.1 GPa, and the

self-consistent field (SCF) convergence tolerance was set to be $2.0\times10^{-6}$ eV/atom.

### 2.2 Computational model

Common pyrite ($FeS_2$) possesses a cubic crystal structure and has a space group of $Pa\bar{3}(T_h^6)$. The common cleavage plane is face (100) along bond Fe—S. Each Fe atom on the surface coordinates with adjacent five S atoms, while each S atom coordinates with adjacent two Fe atoms and one S atom (Fig. 1(a)). Sphalerite has cubic crystal structure with space group of $F-\bar{4}3m$ with surface (110). Each Zn atom of the surface coordinates with three S atoms, while each S atom coordinates with two Zn atoms and one S atom (Fig. 1(b)). Galena (PbS) also belongs to cubic crystal structure with a space group of *Fm*3*m*. Common cleavage plane is face (100) along bond Pb—S. Each Pb atom of the surface coordinates with adjacent five S atoms, and each S atom coordinates with five Pb atoms (Fig. 1(c)). Low chalcocite has an orthorhombic unit cell with a space group of *P*2(1)/*c*, whose slab models surface (100) is shown in Fig. 1(d). S atom of the surface coordinates with four Cu atoms or three Cu atoms, and Cu atom coordinates with three S atoms and one Cu atom, or two S atoms and two Cu atoms, or three S atoms and two Cu atoms. Stibnite crystallizes in an orthorhombic space group (*Pnma*). Common cleavage plane is face (010), whose slab model is shown in Fig. 1(e). S atom of the surface coordinates with two Sb or three Sb atoms, and each Sb atom coordinates with three S atoms. Molybdenite is a hexagonal crystal with a space group of *P*63/*mmc*, whose cleavage plane is (001). Slab model of molybdenite is shown in Fig. 1(f).

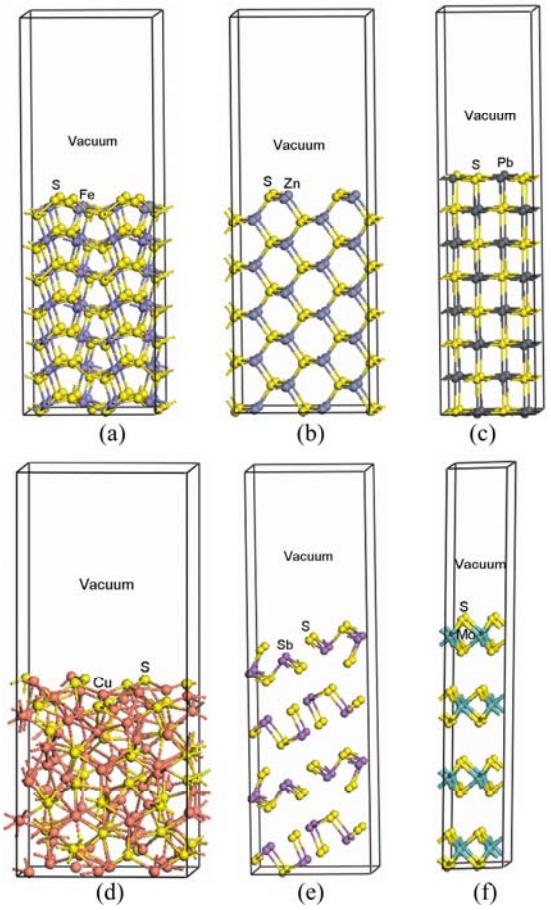


**Fig. 1** Slab models of sulfides: (a) $FeS_2$; (b) ZnS; (c) PbS; (d) $Cu_2S$; (e) $Sb_2S_3$; (f) $MoS_2$

All surfaces were obtained from the bulk sulfides with the optimum unit cell volume and were modeled by a supercell approach (2×2×1) except for chalcocite (1×1×1), where the central cell, periodic in 3D, contains a slab with two surfaces and a vacuum gap above and below the surfaces separating adjacent mirror images of the slab. The surface energies of a range of surfaces with varying slab thicknesses were calculated to determine the slab size. Figure 1 shows the most stable slab models resulted from DFT calculations. During all geometry optimization calculations, the central atomic layer of the slab is kept fixed to prevent the slab from drifting vertically along the supercell.

### 2.3 Calculation of adsorption energy and heat

The adsorption energies of $H_2O$ and $N_2$ on sulfide surfaces are calculated as

$$E_{ads} = E_{x/surface} - E_x - E_{surface} \quad (1)$$

where $E_{ads}$ is the adsorption energy; $E_x$ is the energy of the $H_2O$ or $N_2$ molecules calculated in a cubic cell (x= $H_2O$ or $N_2$); $E_{surface}$ is the energy of the pyrite, sphalerite, galena, chalcocite, stibnite, or molybdenite slab; $E_{x/surface}$ is the energy of the pyrite, galena, sphalerite, chalcocite, stibnite, or molybdenite slab with adsorbed $H_2O$ and $N_2$.

## 3 Results

### 3.1 Interaction between water and surface of sulfide minerals surfaces

There are many adsorption sites for $H_2O$ interaction with sulfide surface. Each adsorption site would provide a lot of important information. To determinate the optimal adsorption site of $H_2O$ on sulfide surfaces which is the most stable structure, adsorption site and adsorption configuration were examined. The calculation results show that the interaction between oxygen of $H_2O$ molecules and metal atom of mineral surfaces is the strongest. Figure 2 shows the adsorption models of $H_2O$ molecules on the surface of pyrite, sphalerite, galena, chalcocite, stibnite and molybdenite, which are the most stable adsorption configuration through optimization test of various adsorption sites.

It is obviously observed from the models in Fig. 2 that $H_2O$ molecules show significantly different

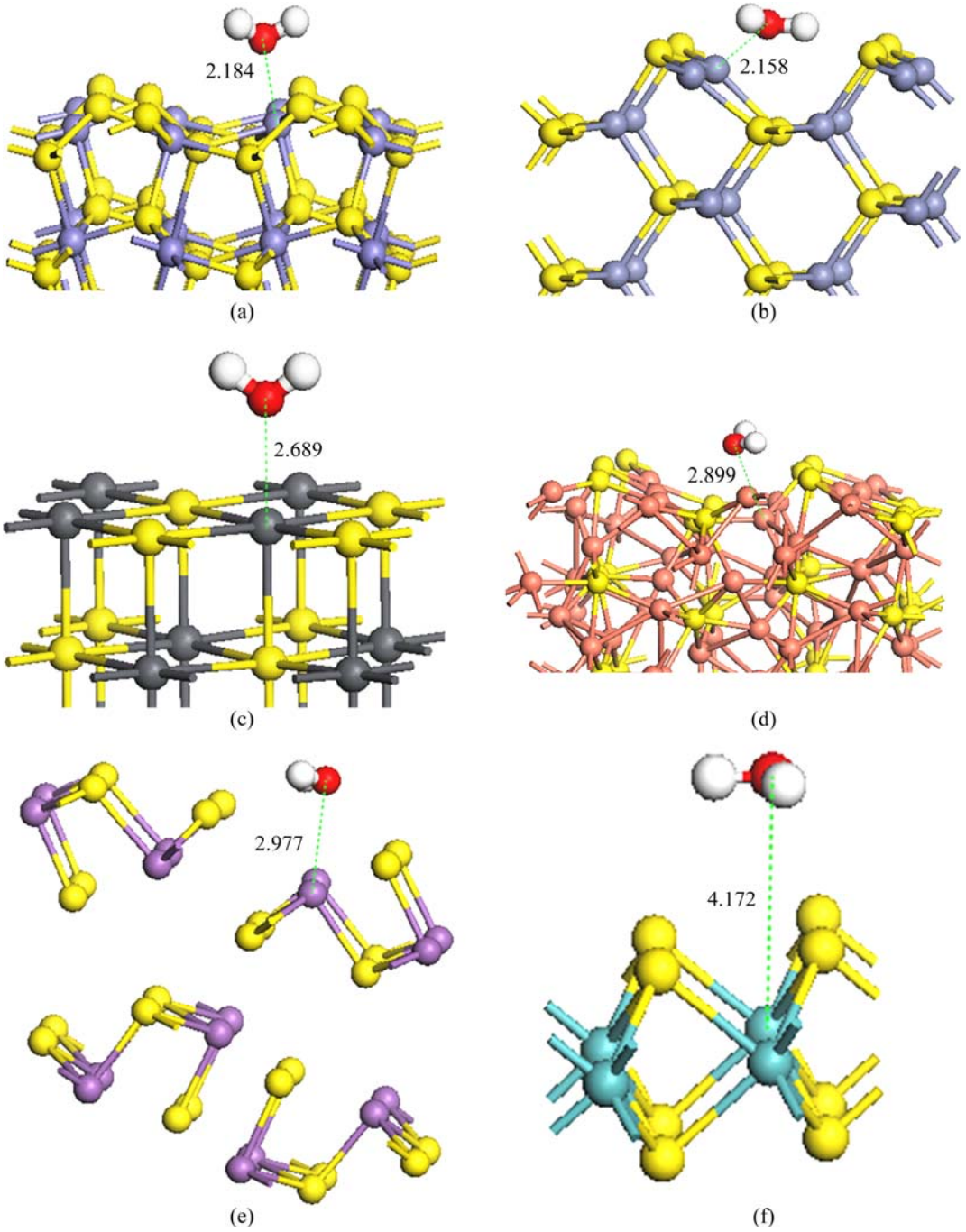


**Fig. 2** Adsorption models of $H_2O$ molecule on various sulfides surfaces (Numbers indicate the distance in Å): (a) $FeS_2$; (b) ZnS; (c) PbS; (d) $Cu_2S$; (e) $Sb_2S_3$; (f) $MoS_2$

adsorption modes on various minerals surfaces. Table 1 presents the distance changes between O atoms of $H_2O$ molecules and adsorption atom (metal) of minerals surfaces ($d_{ads}$) compared with the sum of the atomic radius of O atom and adsorption atom ($d_0$). After adsorption, the distance between O of $H_2O$ molecules and Fe atom of pyrite surface obviously decreases (−0.186 Å), indicating that the strong interaction takes place between $H_2O$ and pyrite surface. The distance between O atoms of $H_2O$ molecules and Zn atom of sphalerite surface slightly changes (−0.022 Å), suggesting weak interactions between $H_2O$ molecules and sphalerite surface. Whereas for the other four sulfides (galena, chalcocite, stibnite, and molybdenite), the distances between O atoms of $H_2O$ molecules and adsorption atoms of all sulfide surfaces after adsorption increase. Among them, the distance change between O atoms of $H_2O$ molecules and Mo atom of molybdenite surfaces is the largest (1.512 Å), then stibnite (0.797 Å), chalcocite (0.679 Å), and galena (0.529 Å) in order,

suggesting that $H_2O$ molecule is repelled by these mineral surfaces. The above results indicate that pyrite and sphalerite are hydrophilic, but galena, chalcocite, stibnite, and molybdenite are hydrophobic.

**Table 1** Variations of distance between O atoms of $H_2O$ and metal atoms of mineral surfaces after adsorption

| Mineral | $d_0(=r_0+r_{metal})$/Å | $d_{ads}$/Å | $\Delta d(=d_{ads}-d_0)$/Å |
|---|---|---|---|
| $FeS_2$ | 2.37 | 2.184 | −0.186 |
| ZnS | 2.18 | 2.158 | −0.022 |
| PbS | 2.16 | 2.689 | 0.529 |
| $Cu_2S$ | 2.22 | 2.899 | 0.679 |
| $Sb_2S_3$ | 2.18 | 2.977 | 0.797 |
| $MoS_2$ | 2.66 | 4.172 | 1.512 |

$r_0$ is atomic radius of O for $H_2O$; $r_{metal}$ is atomic radius of metal for sulfide surface; $d_{ads}$ is the distance between O atom of $H_2O$ and metal atom of mineral surfaces after adsorption.

To assure the strength of interactions between $H_2O$ molecules and sulfide surfaces, the changes of H—O—H angle and H—O bond length of $H_2O$ molecules on sulfide surfaces before and after adsorption were calculated and the data are presented in Table 2. The change of H—O—H angle of $H_2O$ adsorbed on pyrite surface is the largest, and increases from 104.425° to 107°, while change of H—O bond length of $H_2O$ adsorbed on sphalerite surface is the largest, from 0.977 Å to 0.996 Å. These results confirm the strong interaction between $H_2O$ and the surface of pyrite and sphalerite. The changes of H—O—H angle and H—O bond length of $H_2O$ adsorbed on galena, chalcocite, stibnite, and molybdenite surfaces are relatively small, indicating the weak interaction between $H_2O$ and the surfaces.

### 3.2 Adsorption energies of $H_2O$ molecules on sulfide minerals surfaces

Table 3 shows the adsorption energies of $H_2O$ molecules on the surfaces of various sulfide minerals ($E_{H_2O-sulfides}$). The data reveal that the adsorption energy of $H_2O$ on the pyrite surface is the largest, −71.206 kJ/mol; then sphalerite, −24.218 kJ/mol; galena, −8.973 kJ/mol; stibnite, −8.008 kJ/mol; chalcocite, −2.026 kJ/mol; molybdenite, 2.026 kJ/mol (negative sign represents exothermic reaction). The adsorption energy of $H_2O$ on the pyrite surface at low coverage by STIRLING et al [11] is −54.6 kJ/mol (−13 kcal/mol), which is slightly lower than our result (−71.206 kJ/mol). The smaller adsorption energy may be due to different parameters used in the calculations by STIRLING et al [11], such as cut-off energy and vacuum layer. In fact, there also exist interactions between $H_2O$ molecules that affect the adsorption of a $H_2O$ molecule toward the mineral surfaces. The binding energy between $H_2O$ molecules ($E_{H_2O-H_2O}$) was calculated to be −19.297 kJ/mol (Table 3). The data show that the adsorption energies of $H_2O$ molecules on pyrite and sphalerite surfaces are larger than binding energy between $H_2O$ molecules ($\Delta E = E_{H_2O-sulfides} - E_{H_2O-H_2O} < 0$), while the adsorption energies of $H_2O$ on the surfaces of galena, chalcocite, stibnite and molybdenite are smaller than binding energy between $H_2O$ molecules ($\Delta E = E_{H_2O-sulfides} - E_{H_2O-H_2O} > 0$). These results suggest that $H_2O$ molecule prefers to stay with pyrite and sphalerite surfaces rather than water, whereas for galena,

**Table 2** Variations of H—O—H angle and H—O bond length of $H_2O$ molecule on sulfide surfaces before and after adsorption

| Sulfide | Before adsorption | | After adsorption | |
|---|---|---|---|---|
| | H—O—H angle/(°) | H—O bond length/Å | H—O—H angle/(°) | H—O bond length/Å |
| Pyrite ($FeS_2$) | 104.425 | 0.977 | 107 | 0.981 |
| Sphalerite (ZnS) | 104.425 | 0.977 | 105.881 | 0.996 |
| Galena (PbS) | 104.425 | 0.977 | 106.554 | 0.975 |
| Chlorite ($Cu_2S$) | 104.425 | 0.977 | 104.355 | 0.979 |
| Stibnite ($Sb_2S_3$) | 104.425 | 0.977 | 102.357 | 0.979 |
| Molybdenite ($MoS_2$) | 104.425 | 0.977 | 104.331 | 0.977 |

**Table 3** Adsorption energies of $H_2O$ molecules on sulfides surfaces (Negative sign represents exothermic reaction)

| Sulfide | Crystal surface | Adsorption energy/(kJ·mol$^{-1}$) | | |
|---|---|---|---|---|
| | | $E_{H_2O-sulfides}$ | $E_{H_2O-H_2O}$ | $\Delta E = E_{H_2O-sulfides} - E_{H_2O-H_2O}$ |
| Pyrite ($FeS_2$) | (1 0 0) | −71.206 | −19.297 | −52.223 |
| Sphalerite (ZnS) | (1 1 0) | −24.218 | −19.297 | −4.921 |
| Galena (PbS) | (1 0 0) | −8.973 | −19.297 | 10.324 |
| Stibnite ($Sb_2S_3$) | (0 1 0) | −8.008 | −19.297 | 11.289 |
| Chalcocite ($Cu_2S$) | (1 0 0) | −2.026 | −19.297 | 17.271 |
| Molybdenite ($MoS_2$) | (0 0 1) | 2.026 | −19.297 | 21.323 |

chalcocite, stibnite, and molybdenite, $H_2O$ molecule prefers to stay with water rather than the minerals surfaces. These results confirm that pyrite and sphalerite surfaces are hydrophilic, while galena, chalcocite, stibnite, and molybdenite surfaces are hydrophobic. It is obvious that hydrophobic galena, chalcocite, stibnite, and molybdenite provide natural floatability.

To find out whether hydrophilic pyrite and sphalerite are naturally floatable, we selected inert gas $N_2$ as adsorption molecule and studied the adsorption energies of $N_2$ on the surfaces of pyrite and sphalerite (Table 4). Adsorption energy of $N_2$ on pyrite surface (−125.913 kJ/mol) was larger than that of $H_2O$ on pyrite surface (−71.206 kJ/mol). The results suggest that pyrite surface favors gas ($N_2$) more than water; hence, pyrite surface is aerophilic. In other words, pyrite also offers natural floatability. The adsorption energy of $N_2$ on sphalerite surface is 12.370 kJ/mol (positive value), indicating that $N_2$ cannot be adsorbed on the surface of sphalerite. It suggests that sphalerite surface is hydrophilic but aerophilic. As a result, sphalerite does not provide natural floatability. In summary, pyrite, galena, chalcocite, stibnite, and molybdenite have natural floatability, while sphalerite shows no natural floatability, which is in fair agreement with the experimental results presented in Table 5 [9].

**Table 4** Adsorption energies of $H_2O$ and $N_2$ molecules on sulfides surfaces

| Sulfide | Crystal surface | Adsorption energy (kJ·mol$^{-1}$) | |
|---|---|---|---|
| | | $E_{H_2O-sulfides}$ | $E_{N_2-sulfides}$ |
| Pyrite ($FeS_2$) | (1 0 0) | −71.206 | −125.913 |
| Sphalerite (ZnS) | (1 1 0) | −24.218 | 12.370 |

The flotation recovery results in Table 5 reveal that the recoveries of pyrite, galena, chalcocite, stibnite, and molybdenite are greater than 80%, indicating that the surfaces of these sulfides are more hydrophobic than hydrophilic, that is, they provide natural floatability. On the other hand, the recovery of sphalerite is smaller than 60%, indicating that the surface of sphalerite is hydrophilic. According to FUERSTENAU and SABACKY [9], one of the reasons for the differences of these results with those obtained by other researchers is the content of oxygen. Our results confirm this viewpoint.

The reason why pyrite and galena, chalcocite, stibnite, and molybdenite provide natural floatability, while sphalerite is hydrophilic, according to the slab model (Fig. 1), is that galena, stibnite, and molybdenite have layered structure, so their interactions in the direction perpendicular to the surfaces is very weak, which leads to the weak adsorption strength of $H_2O$ on the surfaces of these sulfides, as shown in Table 3. Therefore, galena, stibnite, and molybdenite are naturally floatable. As for pyrite, chalcocite, and sphalerite, we will analyze them later using the density of states (DOS) of adsorption atom for sulfide surfaces.

**Table 5** Flotation recovery of sulfides from various sources (Conditions: particle size of 100×200 mesh, pH = 6.8, no collector, no frother [9])

| Sulfide | Source | Flotation recovery/% |
|---|---|---|
| Galena | Coeur D'Alene, Idaho | 100 |
| | Bixby, Missouri | 100 |
| | Pitcher, Oklahoma | 100 |
| | Galena, South Dakota | 100 |
| Chalcopyrite | Temagami, Ontario | 100 |
| | Sudbury, Ontario | 100 |
| | Beaver Lake District, Utah | 97 |
| | Messina, Transvaal | 93 |
| Chalcocite | Kennecott, Alaska | 100 |
| | Evergreen, Colorado | 88 |
| | Butte, Montana | 86 |
| | Superior, Arizona | 83 |
| Pyrite | Amba Saguas, Spain | 92 |
| | Custer, South Dakota | 85 |
| | Zacatecase, Mexico | 83 |
| | Naica, Mexico | 82 |
| Sphalerite | Keystone, South Dakota | 56 |
| | Joplin, Missouri | 47 |
| | Creede, Colorado | 46 |
| | Pitcher, Oklahoma | 41 |

### 3.3 Density of states of sulfides surface atoms

Figure 3 shows DOS results of metal atoms of sulfide surfaces. The position of Fermi level is 0. For metal and semiconductor, significantly physical processes occur in the vicinity of Fermi level. In other words, DOS at Fermi level represents atomic reaction activity. So, we only considered the details near Fermi surface. It is observed from Fig. 4 that near Fermi level, electrons of $MoS_2$, $Sb_2S_3$, $Cu_2S$, and PbS surfaces are mainly from the Mo 4d, Sb 5p, Cu 3d, and Pb 6p orbitals. However, their DOS is small at Fermi level, especially for $MoS_2$, $Sb_2S_3$, and PbS, which indicates that these sulfides surfaces are inactive. However, it is not easy for them to react with $H_2O$ or absorb $H_2O$ on the surface. As a result, they are hydrophobic in character. In the case of $FeS_2$, compared with other four sulfide minerals, DOS of Fe 3d at Fermi level is large, indicating that pyrite surface is active. Hence, it is easy for pyrite to absorb water, which is in good agreement with its hydrophilicity.

However, it is probable that the interaction of $FeS_2$ with $N_2$ to be stronger than that of $FeS_2$ with $H_2O$, which leads to its natural floatability. To confirm this viewpoint, DOS of surface Fe atom after $H_2O$ and $N_2$ adsorption on pyrite surface was studied. The results are presented in Fig. 4. As for ZnS, the reaction activity does not confirm the rule of semiconductors because of being an insulator [18]; therefore, sphalerite is not discussed here.

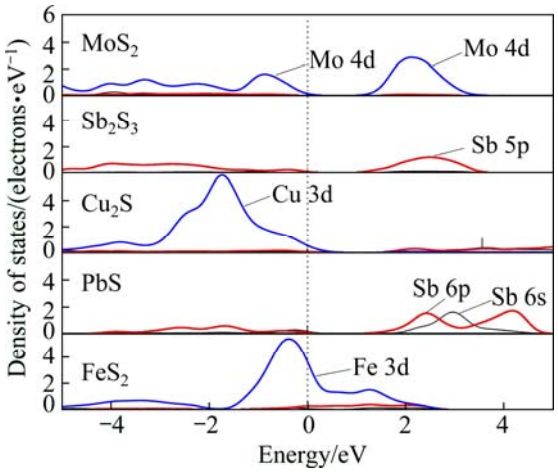


**Fig. 3** DOS results of sulfides surfaces atoms

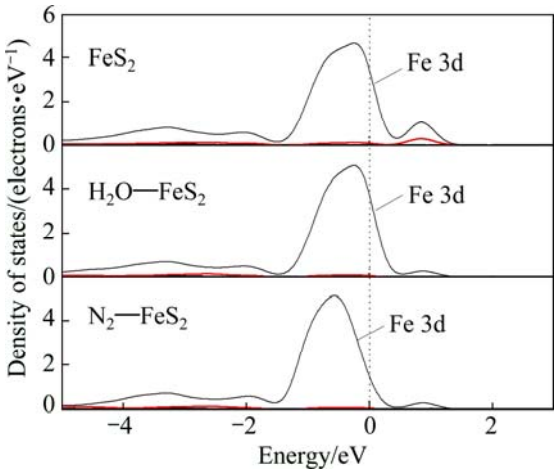


**Fig. 4** DOS results of surface Fe atom for pyrite after $N_2$ and $H_2O$ adsorption

According to plot of Fig. 4, Fe 3d DOS curve of $H_2O$–$FeS_2$ is close to that of pure $FeS_2$ mineral near Femi level, while Fe 3d DOS curve of $N_2$–$FeS_2$ shows obvious difference compared with pure $FeS_2$ mineral. On one hand, the shape of DOS curve of Fe 3d changes, and on the other hand, peak position of Fe 3d DOS shifts to a lower energy level. The results indicate that the reaction of pyrite with $H_2O$ is weaker than that of pyrite with $N_2$. In other words, pyrite tends to be aerophilic ($N_2$) relative to $H_2O$, which confirms the natural floatability of pyrite.

To know why sphalerite is hydrophilic and not aerophilic, DOS values of surface Zn atom after $H_2O$ and $N_2$ adsorption on sphalerite surface were calculated, as shown in Fig. 5. For the convenience of comparison, DOS of Zn atom for pure ZnS mineral surface is also shown in Fig. 5. Plots in this figure show that Zn 3d DOS of $N_2$−ZnS surface approximates to the pure ZnS surface while Zn 3d DOS peak of $H_2O$−ZnS surface clearly shifts to a higher energy level. The results suggest that the interaction between $H_2O$ and sphalerite surface is stronger than that between $N_2$ and sphalerite. As a result, sphalerite tends to be hydrophilic.

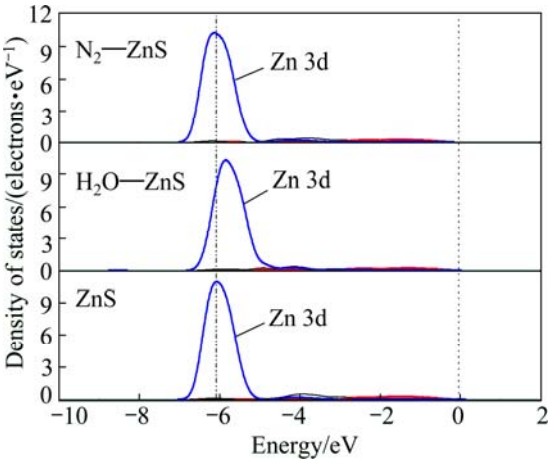


**Fig. 5** DOS results of Zn surface atom for sphalerite after $N_2$ and $H_2O$ adsorption

## 4 Conclusions

1) After adsorption, the distance between O of $H_2O$ molecules and Fe atom of pyrite surface obviously decreases, the distance between O atoms of $H_2O$ molecules and Zn atom of sphalerite surface slightly changes. Whereas for galena, chalcocite, stibnite, and molybdenite, the distances between O atoms of $H_2O$ molecules and adsorption atoms of all sulfide surfaces increase.

2) $H_2O$ molecule prefers to stay with pyrite and sphalerite surfaces rather than water, whereas for galena, chalcocite, stibnite, and molybdenite, $H_2O$ molecule prefers to stay with water rather than the minerals surfaces, which shows that pyrite and sphalerite surfaces are hydrophilic, while galena, chalcocite, stibnite, and molybdenite surfaces are hydrophobic.

3) Pyrite surface favors $N_2$ more than water, while sphalerite surface cannot adsorb $N_2$ and cannot be adsorbed on the surface of sphalerite. Therefore, pyrite surface is aerophilic, while sphalerite surface is hydrophilic but aerophilic.

4) The reaction of pyrite with $H_2O$ is weaker than that of pyrite with $N_2$, while the interaction between $H_2O$ and sphalerite surface is stronger than that between $N_2$ and sphalerite,

## References


[1] RAVITZ S F. Oxygen-free flotation. II—Further experiments with galena [M]. New York: AIME Tech Pub, 1940: 1147−1168.

[2] SUTHERLAND K L, WARK I W. Principles of flotation [M]. Melbourne: Australas Inst Min Metall, 1955.

[3] KLASSEN V I, MOKROUSOV M A. An introduction to the theory of flotation [M]. 2nd ed. London: Butterworths, 1963.

[4] FINKELSTEIN N P, ALLISON S A, LOVELL V M, STEWART B V. Natural and induced hydrophobicity in sulfide mineral systems [C]//SOMASUNDARAN P, GRIEVES R B. Advances in Interfacial Phenomena of Particulate/Solution/Gas Systems. New York: Am Inst Chem Eng, Symp Ser, 1975: 165−175.

[5] LEPETIC V M. Flotation of chalcopyrite without a collector after dry, autogenous grinding [J]. Can Inst Metall Bull, 1974, 67: 71−74.

[6] HEYES G W, TRAHAR W J. The natural floatability of chalcopyrite [J]. Int J Miner Process, 1977, 4: 317−344.

[7] GARDNER J R, WOODS R. An electrochemical investigation of the natural flotability of chalcopyrite [J]. Int J Miner Process, 1979, 6: 1−16.

[8] YOON R H. Collectorless flotation of chalcopyrite and sphalerite ores by using sodium sulfide [J]. Inter J Miner Process, 1981, 8: 31−48.

[9] FUERSTENAU M C, SABACKY B J. On the natural floatability of sulfides [J]. Inter J Miner Process, 1981, 8: 79−84.

[10] ZHAO Cui-hua, CHEN Jian-hua, LONG Xian-hao, GUO Jin. Study of $H_2O$ adsorption on sulfides surfaces and hermokinetic analysis [J]. Journal of Industrial and Engineering Chemistry, 2014, 20(2): 605−609.

[11] STIRLING A, BERNASCONI M, PARRINELLO M. Ab initio simulation of water interaction with the (100) surface of pyrite [J]. The Journal of Chemical Physics, 2003, 118: 8917−8926.

[12] GUEVREMONT J M, STRONGIN D R, SCHOONEN M A A. Photoemission of adsorbed Xenon, X-ray photoelectron spectroscopy, and temperature-programmed desorption studies of $H_2O$ on $FeS_2$ (100) [J]. Langmuir, 1998, 14(6): 1361−1366.

[13] WRIGHT K, HILLIER I H, VAUGHAN D J, VINCENT M A. Cluster models of the dissociation of water on the surface of galena (PbS) [J]. Chemical Physics Letters, 1999, 299(6): 527−531.

[14] ROSSO K M, BECKER U, HOCHELLA M F. The interaction of pyrite {100} surfaces with $O_2$ and $H_2O$: Fundamental oxidation mechanisms [J]. American Mineralogist, 1999, 84: 1549−1561.

[15] PAYNE M C, TETER M P, ALLAN D C, ARIAS T A, JOANNOPOULOS J D. Iterative minimization techniques for ab initio total energy calculation: Molecular dynamics and conjugate gradients [J]. Reviews of Modern Physics, 1992, 64: 1045−1097.

[16] PERDEW J P, WANG Y. Accurate and simple analytic representation of the electron-gas correlation energy [J]. Phys Rev B, 1992, 45: 13244−13249.

[17] VANDERBILT D. Soft self-consistent pseudopotentials in a generalized eigenvalue formalism [J]. Phys Rev B, 1990, 41: 7892−7895.

[18] de GIUDICI G, VOLTOLINI M, MORET M. Microscopic surface processes observed during the oxidative dissolution of sphalerite [J]. European Journal of Mineralogy, 2002, 14(4): 757−762.


# 硫化矿物表面天然疏水性的密度泛函理论研究


赵翠华[1,2,3]，陈建华[1,4]，吴伯增[2]，龙贤灏[1]

1. 广西大学 化学化工学院，南宁 530004；
2. 广西华锡集团股份有限公司，柳州 545006；
3. 广西大学 材料科学与工程学院，南宁 530004；
4. 广西大学 资源与冶金学院, 南宁 530004



**摘　要**：采用密度泛函理论研究了水在硫化矿物表面的吸附以及硫化矿物的天然可浮性。为了排除氧气和其他因素的影响，所有的计算模型都是在真空环境下建立的。水分子是在黄铁矿与闪锌矿的表面，而不是在水里。对于方铅矿、辉铜矿、辉锑矿和辉钼矿，水分子是在水里，而不是在这些矿的表面。另一方面，黄铁矿表面亲氮气而不亲水，而闪锌矿表面不能吸附水。结果表明，方铅矿、辉锑矿、辉铜矿及辉钼矿是疏水的，而闪锌矿是亲水的。黄铁矿具有一定的亲水性，但是它更倾向于亲气，这是因为黄铁矿与水的作用要比与氮气的作用弱。因此，黄铁矿、方铅矿、辉铜矿、辉锑矿及辉钼矿都具有天然可浮性。



**关键词**：硫化矿；水吸附；天然可浮性；密度泛函理论

**(Edited by Hua YANG)**